



Cite this: *Chem. Sci.*, 2020, **11**, 6362

All publication charges for this article have been paid for by the Royal Society of Chemistry

Received 20th February 2020  
 Accepted 11th March 2020

DOI: 10.1039/d0sc01011a  
[rsc.li/chemical-science](http://rsc.li/chemical-science)

## Introduction

Decomposition of diazo compounds in the presence of oxygen, nitrogen, sulfur or phosphorus Lewis bases is a recognized strategy to generate the corresponding ylides efficiently.<sup>1</sup> In the case of oxonium ylides, diazo reagents decomposed under photochemical or metal-catalyzed conditions<sup>2</sup> are known to react with cyclic ethers such as epoxides,<sup>3</sup> oxetane,<sup>4</sup> THF,<sup>5</sup> THP,<sup>6</sup> 1,3- and 1,4-dioxane,<sup>7</sup> or oxepane,<sup>8</sup> and the subsequent intermediates are used in a large panel of reactions including macrocyclization.<sup>7e,9</sup> Macroyclic molecules are an important class of compounds in nature. About 20% of the known natural products are made of a cyclic core with at least 11 atoms.<sup>10</sup> Many of them exhibit a variety of biological<sup>11</sup> or medicinal properties.<sup>12</sup> Polyether macrocycles are a particular subclass of this family that act as efficient binding receptors for cations or small molecules.<sup>13</sup> Attaching a suitable functional group or a probe to the core of the molecule leads to various and versatile uses and applications such as catalysis<sup>14</sup> or sensing for either recognition or quantification of analytes.<sup>15</sup>

However, synthesis of such large and highly functionalized molecules requires several synthetic steps and usually high dilution conditions for the key ring-closure.<sup>16</sup> To circumvent this major drawback, a new type of macrocyclic  $[3 + X + 3 + X]$  condensation ( $X = 5, 6$  or  $7$ ) was developed by Lacour and co-workers based on new diazo decomposition reactivity in the presence of common and simple cyclic ethers. Coupled with an unprecedented tandem [amidation + olefin transposition] sequence, the ylide reactivity then leads to the new and original family of chiral polyether macrocycles **1** (Fig. 1). This mini

## From reactive carbenes to chiral polyether macrocycles in two steps – synthesis and applications made easy?

Alexandre Homberg and Jérôme Lacour \*

Chiral polyether macrocycles are versatile molecules. For their preparation, original two-step procedures were recently developed and present the advantages of high concentration conditions and simple starting reagents (stable diazo reagents, small cyclic ethers, aliphatic or aromatic amines). Enantiopure materials are readily afforded by CSP-HPLC on a semi-preparative scale. Flexibility and adaptability in the macrocyclic design are provided by a large selection of amines to choose from while the ring size and chemical nature are controlled by the choice of 5 to 7-membered cyclic ether precursors. Such macrocycles have already been used as asymmetric catalysts, mono and ditopic receptors, fluorescent sensors and probes, and chiroptical reversible switches.

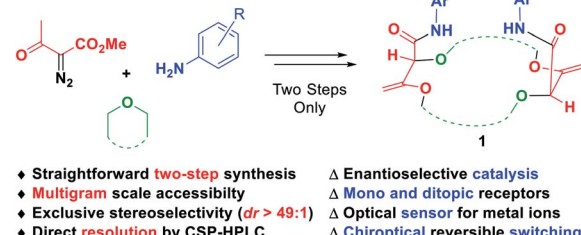


Fig. 1 Straightforward multicomponent synthesis and applications of highly functionalized chiral polyether macrocycles **1**.

review will focus on the unique synthesis of compounds **1** and the various derived applications. First, the key macrocyclization step and subsequent optimizations, which lead to routine synthetic procedures on a large scale (up to 20 gram batches), will be presented. Second, the highly diastereoselective amidation plus transposition process will be detailed. Finally, different applications of such types of macrocycles ranging from catalysis to reversible chiroptical switching will be detailed.

## Chiral polyether macrocycles: synthesis

### Step 1: diazo decomposition towards reactive ylide intermediates and unsaturated macrocycles

Decomposition of diazo compounds by transition metal catalysts is an effective way to generate electrophilic metal carbenes.<sup>1a</sup> These reactive species undergo further transformations

such as dimerization, insertion, cyclopropanation, dipolar addition, ylide formation and subsequent rearrangement depending on conditions. Ylides, in particular, oxonium ylides, are formed by reaction of metal carbenes with ether moieties.<sup>3,4,7a,17</sup> In this context, 16- to 20-membered ring polyether macrocycles can be synthesized by  $[3 + X + 3 + X]$  multicomponent condensation of methyl  $\alpha$ -diazo- $\beta$ -ketoester 2 with cyclic ethers ( $X = 5$  to 7) under dirhodium(II) catalysis (Fig. 2, top).<sup>7b</sup> Contrary to conventional macrocycle synthesis, this transformation occurs at a high concentration of reagent 2 ( $c 1\text{ M}$ ) and under strictly non-templated conditions. Mechanistically, diazo 2 is decomposed by the dirhodium catalyst to form an electrophilic metal carbene A (Fig. 2, bottom). The cyclic ether then acts as a nucleophile and generates metal-bond oxonium ylide B. After release of the catalyst, (metal-free) oxonium ylide C dimerizes in a non-concerted process to form macrocycle 3.<sup>18</sup> The need for high concentration is explained by this last step which is rate determining and second-order in ylide C kinetically. In addition, the reaction tolerates various  $\alpha$ -diazo- $\beta$ -ketoester reagents to afford the corresponding macrocycles in moderate to good yields (up to 80% generally).<sup>7b</sup>

Also, 1,4-dioxane can be replaced by other 5-, 6- or 7-membered cyclic ethers such as THF (tetrahydrofuran), THP (tetrahydropyran) or oxepane to generate products 3a–3d (Fig. 3).<sup>6</sup> Functionalized THF and THP reagents can also be used to yield densely functionalized 16- and 18-membered ring macrocycles in moderate to good yields (35–67%). The kinetics of the diazo decomposition of 2 was studied with different rhodium catalysts by means of *in situ* infrared (reactIR) monitoring. The  $\text{Rh}_2(\text{OAc})_4$  catalyst used originally was shown to induce the slowest reaction rates for the diazo decomposition ( $0.24\text{ h}^{-1}$ ). Changing the catalytic complex to  $\text{Rh}_2(\text{Oct})_4$  or  $\text{Rh}_2(\text{R-DOSP})_4$  increased the reaction rate by a factor of two (0.54

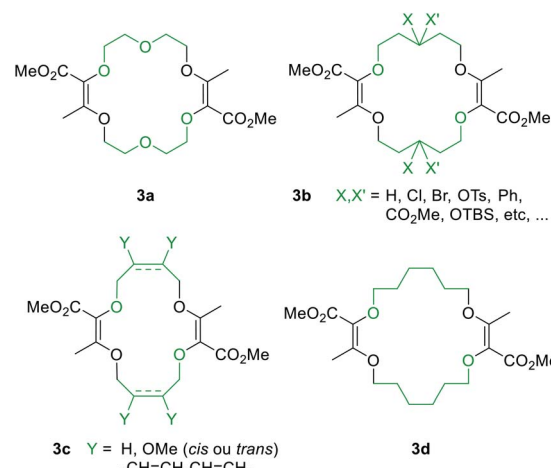


Fig. 3 Macrocycles accessible from regular or functionalized 1,4-dioxane (3a), THP (3b), THF (3c) or oxepane (3d).

$\text{h}^{-1}$  and 0.55  $\text{h}^{-1}$ ). But Hashimoto–Ikegami catalysts,  $\text{Rh}_2(\text{S-TCPTTL})_4$  and  $\text{Rh}_2(\text{S-PTTL})_4$ , showed the highest activity in the decomposition of diazo 2 with first-order kinetic constants of 2.63  $\text{h}^{-1}$  and 3.39  $\text{h}^{-1}$  respectively. Thanks to this higher reactivity and additional speciation studies, it was possible to decrease the amount of catalyst down to  $10^{-3}\text{ mol\%}$  and perform the macrocyclization on a multigram scale.<sup>19</sup> Consequently, by using achiral phthalimido-based cyclohexyl-derived  $\text{Rh}_2(\text{TCPTCC})_4$  ( $10^{-3}\text{ mol\%}$ ), the polyether macrocycle 3a was satisfactorily synthesized in 72% yield (Fig. 4). These optimizations lead to the routine synthesis of 3a on a large scale, up to 20 grams per batch.<sup>19</sup>

Alternatively, protected morpholines were also considered. Such N-containing cyclic ethers react slower with metal carbenes than 1,4-dioxane, THP or THF derivatives (regular path A → B). A competitive Wolff rearrangement of the metal carbene A can occur instead (pathway A → 4, Fig. 2). A ketene intermediate is generated that reacts with a “second” metal carbene A to form compound 4, which is composed of a dioxolene ring fused with an  $\alpha,\beta$ -unsaturated ester moiety. This process is detrimental to macrocycle formation. It was found that an intermediate catalyst loading ( $0.1\text{ mol\%}$ ) favors the O-ylide formation (A → B, Fig. 2) and hence, following the same

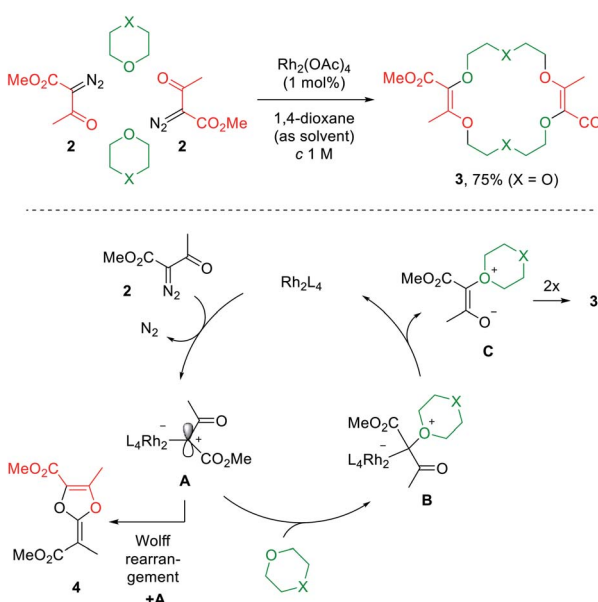


Fig. 2 One pot  $[3 + X + 3 + X]$  condensation of diazo 2 with a cyclic ether under  $\text{Rh}(\text{II})$  catalysis (top) and the proposed mechanism (bottom).

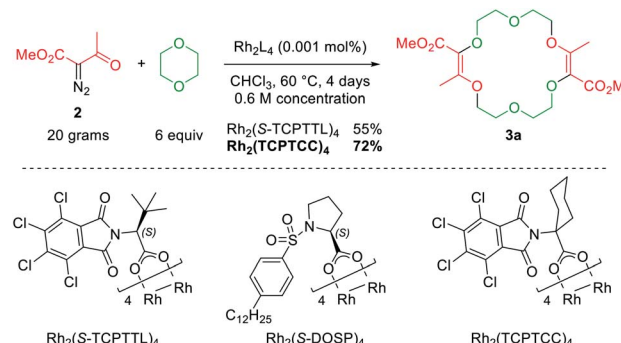


Fig. 4  $[3 + 6 + 3 + 6]$  macrocyclization on a multigram scale.



dimerization mechanism, diaza-macrocycles were satisfactorily afforded in moderate to good yields.<sup>20</sup>

### Step 2: tandem [amidations + olefin transpositions] towards chiral polyether macrocycles

Despite the structural resemblance of compounds **3** to crown ethers, these unsaturated macrocycles do not bind cations. In **3a** for instance, the lone pairs of oxygen atoms are not favorably oriented for cation binding.<sup>7b</sup> The twofold conjugated enol ester systems enforce strong molecular constraints and prevent any efficient structural rearrangement. A protocol was then developed to transform derivatives **3** into chiral frameworks by treatment with an excess of aromatic amines under strongly basic conditions (Fig. 5).<sup>21</sup> In this single one-pot process two transformations occur: (i) the amidation of the ester functions and (ii) the transposition of the olefins from endocyclic to exocyclic positions. This double and tandem [amidation + olefin transposition] process is a highly diastereoselective reaction (diastereomeric ratio  $dr > 49 : 1$ ) as only the chiral (racemic) isomers **1** are formed; achiral (*meso*) diastereoisomers are never observed.

Polyether macrocycles of type **1** possess a peculiar conformation. The crown ether core is almost planar and acts as a platform while the systems formed by the olefins and C–H groups at the stereogenic center forced the two amide substituents to orient orthogonally to the plane of the skeleton to minimize allylic 1,3-strain (Fig. 6). Consequently, the two aromatic moieties are favorably and closely located facing each other. In the case of macrocycles made from 1,4-dioxane like **1a**, a water molecule is also complexed within the polyether macrocyclic core and the amide functions are linked by hydrogen bonding interactions. This transformation is quite general (moderate to good yields) in terms of aromatic amine reagents as electron-rich or -poor anilines, extended aromatic amines and heteroaromatic amines are tolerated in this transformation. Additionally, unsaturated macrocycles made of different skeletons (from THF or THP) also yield the same type of chiral macrocycle after the double tandem [amidation + olefin transposition] process.<sup>22</sup>

With these new chiral macrocycles in hand, a general and practical protocol was developed to resolve derivatives **1** into single enantiomers efficiently by chiral stationary phase (CSP) HPLC. It was found that CHIRALPAK® IG is a particularly effective CSP. Its use, together with eluents in which the macrocyclic derivatives are (highly) soluble such as CH<sub>3</sub>CN and

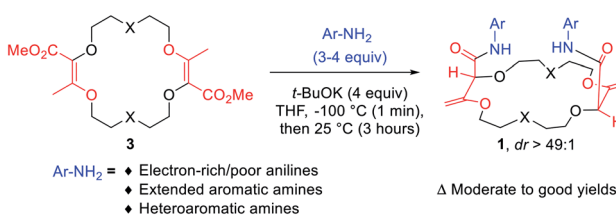


Fig. 5 One pot twofold tandem [amidation + olefin transposition] process.

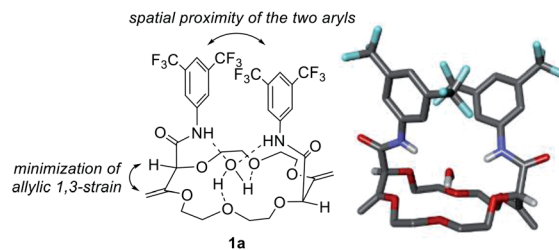


Fig. 6 Solid-state conformation and stick view of the crystal structure **1a**.

CH<sub>2</sub>Cl<sub>2</sub>, renders the enantiomeric separation operational routinely on a semi-preparative scale. Good selectivity factors ( $\alpha$ ) and pure samples of both enantiomers have always been obtained so far.<sup>23</sup>

Alternatively, to obtain macrocycles of type **1** bearing aliphatic amides, a two-step (consecutive) process is required from **3**. In this case, it is necessary to decouple (i) the amidation realized by addition of aliphatic amines in the presence of TBD (1,5,7-triazabicyclo[4.4.0]dec-5-ene) from (ii) the olefin transposition step that is still performed under strongly basic conditions.<sup>24</sup> Various linear and  $\alpha$ -branched primary amines can be introduced and afford chiral aliphatic macrocycles in moderate to good yields. Of interest, it is possible to introduce enantiopure amines that lead to mixtures of diastereoisomers separable by simple flash chromatography and then obtain diastereomerically (and enantiomerically) pure compounds.

The functionalization of the enol ether termini of derivatives **1** was also achieved recently under radical conditions. Double thiol-ene reactions were performed under photo-irradiation. The fully regioselective anti-Markovnikov procedure yields saturated chiral macrocycles with protected or free dithiol arms, with moderate to excellent diastereoselectivity.<sup>25</sup>

## Chiral polyether macrocycles: applications

### Cation binding: catalysis and cooperativity

While solid state structures of macrocycles **1a** (Fig. 6) indicated that the binding of a neutral molecule was possible (e.g. water),<sup>21a</sup> the coordination of cations like Na<sup>+</sup> within the cavity of the polyether macrocycles was evidenced by X-ray crystallography during the preparation of the compounds.<sup>24</sup> This ability to complex alkali metal salts and render them soluble in non-polar solvents can be put to use in efficient phase transfer catalysis (PTC) protocols. In fact, using non-racemic crown ether macrocycles, it is possible to achieve enantioselective alkylation, 1,4-addition or oxidation.<sup>14a–e</sup> Compounds of type **1** bearing enantiopure amide substituents were thus tested as catalysts for asymmetric PTC. The alkylation of protected glycine **5** with benzyl bromide, which affords chiral phenylalanine derivatives **6** as products, was selected as the benchmark.<sup>14d,e</sup> After optimization of the reaction conditions (catalyst, solvent, metal salt, concentration, ...), macrocycle (*S,S,S,S*)-**1b** was found to be the best catalyst for this transformation.



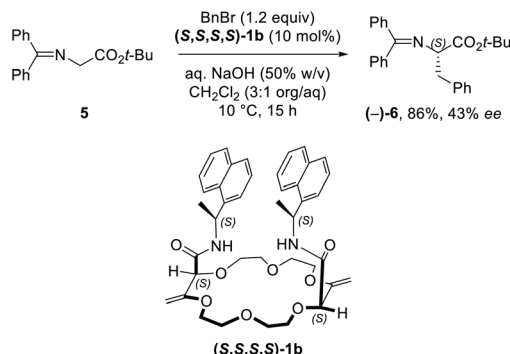


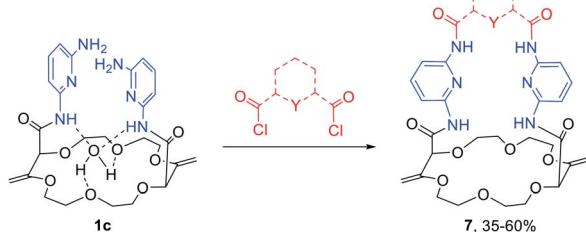
Fig. 7 Asymmetric phase-transfer catalysis with diastereomerically pure **1b** as the catalyst.

Optically active protected phenylalanine  $(-)$ -**6** was afforded in 86% yield and 43% *ee* (Fig. 7).<sup>24</sup>

Knowing that macrocycles of type **1** can bind cations, the addition of complementary anion binding sites was further considered. The ditopic receptor formation was realized in a single synthetic step using amino-substituted derivative **1c**. In fact, treatment of precursors **1c** with dicarbonyl dichloride reagents afforded macrocycles **7** in moderate to good yields (35–60%, Scheme 1).<sup>26</sup> Binding properties of this new class of cryptands towards monovalent alkali cations, common anions and combined salts were studied in solution by  $^1\text{H}$  NMR spectroscopy and by X-ray diffraction analysis for solid state structures. Compounds **7** were found to be cooperative heteroditopic receptors for salts as the presence of both cations and anions is needed for favorable interactions. The cryptands present a general ion pair binding capacity towards salts made of monovalent cations ( $\text{Na}^+$ ,  $\text{K}^+$ ) and linear triatomic anions ( $\text{N}_3^-$ ,  $\text{NCO}^-$ ,  $\text{SCN}^-$ ) or a trigonal oxyanion ( $\text{NO}_3^-$ ) in particular. The salts are cooperatively bound within the polyamide-crown ether conjugates as contact ion pairs. The anions are generally complexed within the cavity through the NH bonding interactions while the cations lie encapsulated inside the polyether ring (Fig. 8).

### Luminescence quenching monitoring

Detection and sensing of metal ions are essential for the analysis of biological, chemical and environmental processes.<sup>15d,27</sup> In the previous section, we used NMR spectroscopy and solid state structural analysis to monitor the interactions with salts.



Scheme 1 Synthesis of novel heteroditopic cryptands **7**.

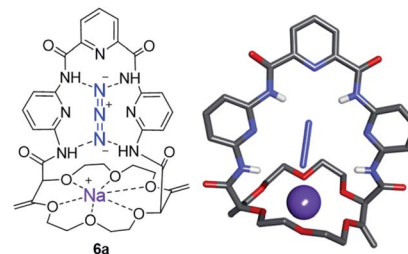


Fig. 8 Stick view of the crystal structure of  $[\text{NaN}_3 \cdot 7\text{a}]$ . Reproduced from ref. 26 with permission from John Wiley and Sons.

An alternative method was to use absorbance and fluorescence techniques<sup>28</sup> which present the advantage of being highly sensitive (micro to nanomolar detection).<sup>29</sup> These methods require the presence of an efficient reporting unit (e.g. fluorophore). One popular fluorophore is the pyrene moiety which exhibits a characteristic emission band at *ca.* 380–400 nm. In the case of spatial proximity between two (or more) pyrene units, a tell-tale excimer fluorescence (EF) centered at 500 nm is observed. The intensity of this transition strongly depends on the distance and the orientation between the two aromatic moieties.<sup>30</sup> In fact, macrocycles of type **1** (bearing fluorophores like pyrene, perylene, fluorene, *etc.*) exhibit intense EF (Fig. 9).<sup>23,31</sup> It was observed that the fluorescence of **1** can be quenched by addition of a metal ion. It was proposed that the amide C=O bonds turn inwards in the presence of such cations

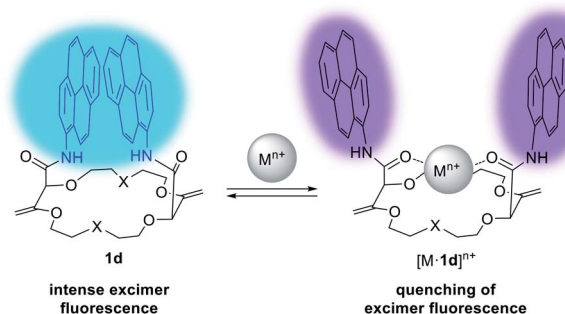


Fig. 9 Fluorescence tuning and proposed conformational changes upon cation binding for **1d**. Reproduced from ref. 31 with permission from John Wiley and Sons.

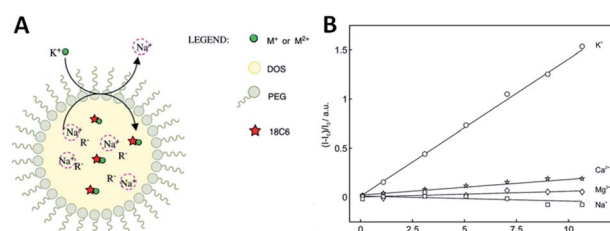


Fig. 10 (A) Ion-selective reverse micelles; (B) normalized fluorescence (406 nm) as a function of concentrations of different cations for **1d**. Reproduced from ref. 8 with permission from the Royal Society of Chemistry.

to favor the complexation. The environment of the aromatic units is thus modified with the two chromophores parting from each other and elongating the distance between them. Hence, the EF is (partially) quenched and only the characteristic emission of (monomeric) the fluorophore is observed.

Using polyether macrocycles **1d**, a systematic analysis of the binding properties of a large range of mono-, di- and trivalent cations (alkaline, alkaline earth, p-, d-, and f-block metals) was performed by means of UV-Vis spectrophotometric titrations, cyclic voltammetry, excimer fluorescence quenching and transient absorption spectroscopy experiments.<sup>31</sup> This study demonstrated that the best binding constants and most efficient quenching of EF are obtained with divalent cations ( $\text{Ba}^{2+}$  and  $\text{Ca}^{2+}$  specifically) in acetonitrile, while monovalent cations ( $\text{Na}^+$  and  $\text{K}^+$  specifically) afford similar results in  $\text{CH}_2\text{Cl}_2$ .<sup>23</sup> Interestingly, the EF properties could also be used for the direct sensing of cations in competitive aqueous media. Reverse micelles composed of bis(2-ethylhexyl) sebacate (DOS), PEG,  $\text{NaBAR}_\text{F}$  and the pyrene derivative **1d** were designed and prepared (Fig. 10A). Using excimer fluorescence quenching, these pH independent nanosensors allowed the sensing of potassium ions after exchange with the sodium contained within the micelle. An acute selectivity for the potassium ion over other metal ions (e.g.  $\text{Na}^+$ ,  $\text{Mg}^{2+}$ ,  $\text{Ca}^{2+}$ ) was demonstrated with the 1,4-dioxane-based **1d** ( $\text{X} = \text{O}$ ) macrocycle in particular (Fig. 10).<sup>8</sup>

It is worth mentioning that cyclometalated dinuclear platinum(II) complexes **1e** (Fig. 11) also present interesting phosphorescence properties. Derivatives **1e** display  $^3\text{MMLCT}$ -based emission originating from an intramolecular Pt–Pt interaction centered around 595 nm. Upon addition of potassium ions and conformation rearrangement (Fig. 9), the dominant emission decreases in intensity while the blue shifted  $^3\text{LC}$  emission increases. The cation can be removed from the macrocycle by addition of regular 18-crown-6, making this system a reversible ratiometric luminescent switch.<sup>32</sup>

Perylene substituted macrocycles **1f** were also used as convenient scaffolds to study targeted photophysical properties, such as symmetry breaking charge separation. The study was performed using stationary and ultrafast electronic spectroscopies combined with molecular dynamics simulations. It was demonstrated that the nature of the excited state varies greatly from an excimer to a symmetry-broken charge separated state depending on the conformational restrictions (cation binding) and the local environment.<sup>33</sup>

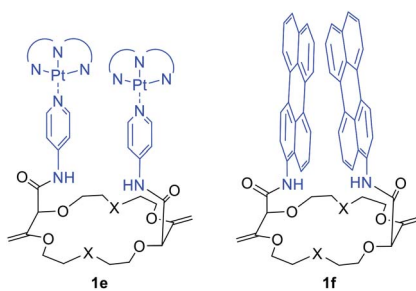


Fig. 11 Macrocycles **1e** and **1f** used as reversible ratiometric luminescent switches and scaffolds to study targeted photophysical properties, respectively.<sup>32,33</sup>

## Effective chiroptical properties

In the previous section, as applications did not require any asymmetric purposes, macrocycles **1a** to **1f** were utilized in the racemic form only. For the following uses, in contrast, care was taken to separate the chiral derivatives into single enantiomers by CSP-HPLC. In fact, a series of fluorescent macrocycles of type **1** substituted with pyrene (**1d**), perylene (**1f**), fluorene or naphthalene monoimide moieties (exhibiting intense excimer fluorescence in different spectral regions) were synthesized and resolved. Their chiroptical properties were then studied using electronic circular dichroism (ECD) and circularly polarized luminescence (CPL) in the absence and in the presence of metal ions.<sup>23</sup> A sign inversion and enhancement of the ECD signal(s) were demonstrated for all derivatives upon addition of cations like  $\text{Na}^+$  or  $\text{Ba}^{2+}$ . Time-dependent density functional theory (TDDFT) calculations were performed to determine the absolute configurations of the derivatives. The simulations also explained the origin of the signal inversions and enhancements. In compounds **1**, the coexistence of multiple conformations with reciprocal arrangements of the amide moieties led

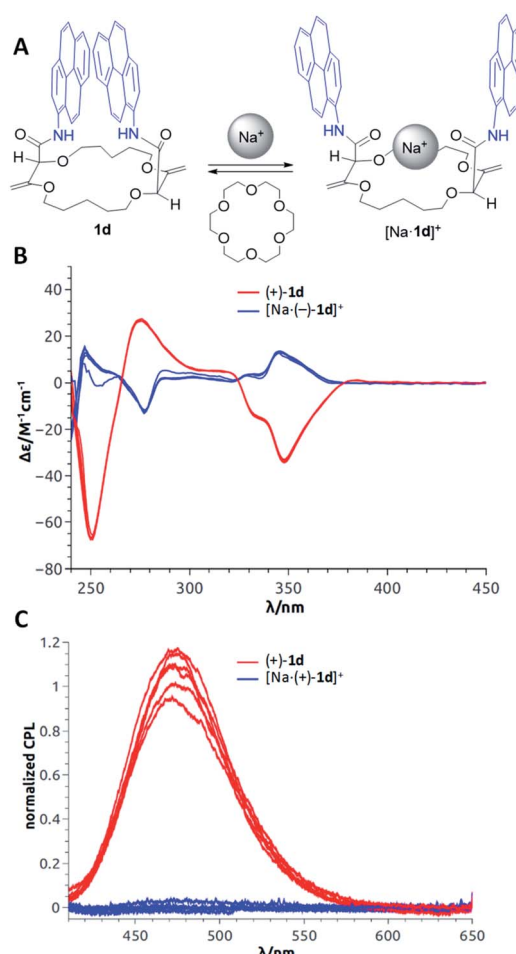


Fig. 12 (A) Model for reversible switching; (B) reversible ECD of  $(+)-1\text{d}$  and  $[\text{Na-}(-)-1\text{d}]^+$  over 6 cycles; (C) reversible CPL of  $(-)-1\text{d}$  and  $[\text{Na-}(-)-1\text{d}]^+$  over 6 cycles. Reproduced from ref. 23 with permission from the Royal Society of Chemistry.

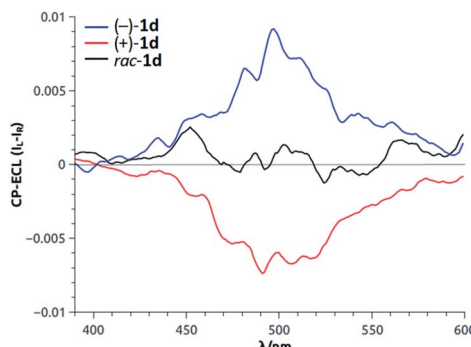


Fig. 13 CP-ECL of **1d** (both enantiomers and racemic mixture). Reproduced from ref. 34 with permission from John Wiley and Sons.

to ECD transitions cancelling each other. However, upon cation addition and binding, the overall number of conformations decreased and the novel conformationally-constrained geometries favored the inverted ECD signal(s) leading to the observed enhancement (Fig. 12B). In emission, strong CPL signals ( $g_{\text{Lum}}$  up to  $10^{-2}$ ) were recorded for the macrocycles associated with excimer fluorescence (Fig. 12C). They are among the highest reported CPL values for single (non-aggregated) and purely organic molecules. Upon cation addition, as in luminescence, the CPL signal was completely quenched because of the conformational rearrangement that disfavored the EF. To induce reversibility, regular 18-crown-6 can be added as a cation scavenger (Fig. 12A),<sup>32</sup> and this led to complete recovery of the original ECD or CPL signals of the “naked” derivatives **1**. The sequence of cation addition and removal can be repeated over several cycles making the reversible system an effective and rare example of allied  $\pm$  ECD and on/off CPL switches (Fig. 12).<sup>23</sup>

Recently, the ability of enantiopure macrocycle **1d** to display intense circularly polarized (CP) luminescence was used in the field of electrochemiluminescence (ECL). Upon electrochemical excitation, enantiomers of **1d** emitted intense CP-ECL with a dissymmetry factor of  $|8 \times 10^{-3}|$  (Fig. 13).<sup>34</sup> This is, in fact, the first example of circularly polarized electrochemiluminescence from a purely organic molecule.

## Conclusion

The catalytic two-step synthesis of macrocycles **1**, starting from simple building blocks (diazo, small cyclic ether and amine), has been highlighted in this mini-review. First, multicomponent  $[3 + X + 3 + X]$  condensation of diazo **2** with small cyclic ethers affords, under dirhodium(II) catalysis (down to 0.001 mol%) and high concentration conditions, unsaturated precursor **3** on a multigram scale. Second, a straightforward double tandem [amidation + olefin transposition] procedure yields chiral macrocycles **1** with excellent stereoselectivity ( $dr > 49 : 1$ ). Applications in a multitude of fields have been found and reported. Compounds **1** have been used for asymmetric PTC and the preparation of scalemic phenylalanine **5**. The cooperative recognition of salts was also achieved using novel ditopic cryptands **6** made in one step from **1c**. The optical

properties of derivatives **1** are also interesting as they allow the direct detection and quantification of metal ions and the development of reversible ratiometric luminescent switches. Thanks to strong chiroptical properties, reversible allied  $\pm$  ECD and on/off switches were efficiently designed. Finally, the first observation of circularly polarized electrochemiluminescence from a purely organic molecule was presented using **1d**.

## Perspectives

Finally, in the following paragraphs, we will try to draw some possible lines of future research – with all the limits that such an exercise encounters.

In terms of synthesis, a direct access to macrocycles larger than 20-membered rings would be ideal for applied projects. However, so far, attempts at using medium-sized rings or traditional crown ethers as substrates, such as the regular 18-C-6, have failed. This is most probably due, in part, to the conformations of these moieties that favor intratoroidal arrangements of the ether oxygen atoms rendering their lone pairs inaccessible. Conditions will have to be found to generate reactive metal carbenes in the immediate proximity of intracyclic heteroatoms for future developments. Care should also be taken to find conditions to perform the tandem [amidation + olefin transposition] in an enantio- and diastereo-selective manner. In fact, while CSP-HPLC conditions provide a reliable and effective means to generate macrocycles **1** as single enantiomers, the process remains limited to the production of scalemic compounds on the milligram scale up to now.

In terms of applications, the distinctive geometry of compounds **1** should be further harnessed. The spatial proximity of the amide arms ought to lead to effective divalent recognition and activation phenomena, and hence to further applications related not only to supramolecular chemistry and spectroscopy but also to enantioselective catalysis. The functionalization of the enol ether groups of derivatives **1** should also remain a priority as the introduction of terminal thiols or carboxylic acid moieties opens an orthogonal chemical space that ought to be useful, for instance, in the manipulation of metal clusters and surfaces.

## Conflicts of interest

There are no conflicts to declare.

## Acknowledgements

We thank the University of Geneva and the Swiss National Science Foundation for financial support (SNF 200020-172497 and 200020-184843). We thank Dr Pilar Franco and Mrs Assunta Green (Chiral Technologies, Illkirch, France) for their help and advice concerning the use of CSP. The group is indebted to the many contributions from fellow collaborators who have participated previously in the diazo decomposition chemistry study and, in this chiral macrocycle domain, we would like to specifically mention Dr Elodie Brun, Dr Radim Hrdina, Dr



Sumit Kumar Ray, Mr Daniele Poggiali, Mr Mahesh Vishe, Dr Walid Zeghida and Dr Francesco Zinna.

## Notes and references

1 (a) M. P. Doyle and M. A. McKervey, *Modern Catalytic Methods for Organic Synthesis with Diazo Compounds: From Cyclopropanes to Ylides*, John Wiley & Son, Ltd., New York, 1998; (b) J. S. Clark, *Nitrogen, Oxygen, and Sulfur Ylide Chemistry: A Practical Approach in Chemistry*, 2002; (c) A. Ford, H. Miel, A. Ring, C. N. Slattery, A. R. Maguire and M. A. McKervey, *Chem. Rev.*, 2015, **115**, 9981–10080; (d) G. K. Murphy, C. Stewart and F. G. West, *Tetrahedron*, 2013, **69**, 2667–2686; (e) H. M. L. Davies and D. Morton, *Chem. Soc. Rev.*, 2011, **40**, 1857–1869; (f) M. P. Doyle, R. Duffy, M. Ratnikov and L. Zhou, *Chem. Rev.*, 2010, **110**, 704–724; (g) A. Padwa, *Chem. Soc. Rev.*, 2009, **38**, 3072–3081; (h) Y. Zhang and J. Wang, *Chem. Commun.*, 2009, 5350–5361; (i) Z. Zhang and J. Wang, *Tetrahedron*, 2008, **64**, 6577–6605; (j) A. Padwa, *Helv. Chim. Acta*, 2005, **88**, 1357–1374; (k) H. M. L. Davies and R. E. J. Beckwith, *Chem. Rev.*, 2003, **103**, 2861–2904; (l) D. M. Hodgson, F. Y. T. M. Pierard and P. A. Stupple, *Chem. Soc. Rev.*, 2001, **30**, 50–61; (m) M. P. Doyle and D. C. Forbes, *Chem. Rev.*, 1998, **98**, 911–936; (n) A. Padwa and M. D. Weingarten, *Chem. Rev.*, 1996, **96**, 223–270; (o) T. Ye and M. A. McKervey, *Chem. Rev.*, 1994, **94**, 1091–1160; (p) M. P. Doyle, *Acc. Chem. Res.*, 1986, **19**, 348–356.

2 A. Padwa and S. F. Hornbuckle, *Chem. Rev.*, 1991, **91**, 263–309.

3 T. Achard, C. Tortoreto, A. I. Poblador-Bahamonde, L. Guénée, T. Bürgi and J. Lacour, *Angew. Chem., Int. Ed.*, 2014, **53**, 6140–6144.

4 (a) L. Egger, L. Guénée, T. Bürgi and J. Lacour, *Adv. Synth. Catal.*, 2017, **359**, 2918–2923; (b) M. Kitamura, M. Kisanuki, K. Kanemura and T. Okauchi, *Org. Lett.*, 2014, **16**, 1554–1557; (c) D. Rix, R. Ballesteros-Garrido, W. Zeghida, C. Besnard and J. Lacour, *Angew. Chem., Int. Ed.*, 2011, **50**, 7308–7311; (d) W. Kirmse and R. Lelgemann, *Chem. Ber.*, 1991, **124**, 1865–1866; (e) W. Kirmse, R. Lelgemann and K. Friedrich, *Chem. Ber.*, 1991, **124**, 1853–1863; (f) K. Friedrich, U. Jansen and W. Kirmse, *Tetrahedron Lett.*, 1985, **26**, 193–196.

5 (a) C. Tortoreto, T. Achard, W. Zeghida, M. Austeri, L. Guénée and J. Lacour, *Angew. Chem., Int. Ed.*, 2012, **51**, 5847–5851; (b) E. Ihara, Y. Hara, T. Itoh and K. Inoue, *Macromolecules*, 2011, **44**, 5955–5960.

6 M. Vishe, R. Hrdina, L. Guénée, C. Besnard and J. Lacour, *Adv. Synth. Catal.*, 2013, **355**, 3161–3169.

7 (a) R. Ballesteros-Garrido, D. Rix, C. Besnard and J. Lacour, *Chem.-Eur. J.*, 2012, **18**, 6626–6631; (b) W. Zeghida, C. Besnard and J. Lacour, *Angew. Chem., Int. Ed.*, 2010, **49**, 7253–7256; (c) E. Ihara, K. Saiki, Y. Goto, T. Itoh and K. Inoue, *Macromolecules*, 2010, **43**, 4589–4598; (d) W. Zhang, X. Shao, L. Yang, Z.-L. Liu and Y. L. Chow, *J. Chem. Soc., Perkin Trans. 2*, 2002, 1029–1032; (e) S. Cenini, G. Cravotto, G. B. Giovenzana, G. Palmisano and S. Tollari, *Tetrahedron*, 1999, **55**, 6577–6584.

8 Z. Jarolímová, M. Vishe, J. Lacour and E. Bakker, *Chem. Sci.*, 2016, **7**, 525–533.

9 (a) D. M. Hodgson and D. Angrish, *Chem.-Eur. J.*, 2007, **13**, 3470–3479; (b) T. M. Weathers, Y. Wang and M. P. Doyle, *J. Org. Chem.*, 2006, **71**, 8183–8189; (c) M. P. Doyle, C. S. Peterson, M. N. Protopopova, A. B. Marnett, D. L. Parker, D. G. Ene and V. Lynch, *J. Am. Chem. Soc.*, 1997, **119**, 8826–8837; (d) M. P. Doyle, C. S. Peterson and D. L. Parker Jr, *Angew. Chem., Int. Ed.*, 1996, **35**, 1334–1336.

10 F. Davis and S. Higson, *Macrocycles: Construction, Chemistry and Nanotechnology Applications*, John Wiley & Son, Ltd., Chichester, U.K., 2011.

11 (a) E. M. M. Abdelraheem, S. Shaabani and A. Dömling, *Synlett*, 2018, **29**, 1136–1151; (b) F. Kopp and M. A. Marahiel, *Nat. Prod. Rep.*, 2007, **24**, 735–749.

12 (a) J. Mallinson and I. Collins, *Future Med. Chem.*, 2012, **4**, 1409–1438; (b) E. M. Driggers, S. P. Hale, J. Lee and N. K. Terrett, *Nat. Rev. Drug Discovery*, 2008, **7**, 608; (c) L. A. Wessjohann, E. Ruijter, D. Garcia-Rivera and W. Brandt, *Mol. Diversity*, 2005, **9**, 171–186; (d) T. Walsh Christopher, *ChemBioChem*, 2002, **3**, 124–134.

13 L. K. S. von Krbek, C. A. Schalley and P. Thordarson, *Chem. Soc. Rev.*, 2017, **46**, 2622–2637.

14 (a) Z. Rapi, T. Nemesok, P. Bagi, G. Keglevich and P. Bakó, *Tetrahedron*, 2019, **75**, 3993–4004; (b) R. Schettini, M. Sicignano, F. De Riccardis, I. Izzo and G. Della Sala, *Synthesis*, 2018, **50**, 4777–4795; (c) J. Tan and N. Yasuda, *Org. Process Res. Dev.*, 2015, **19**, 1731–1746; (d) S. Shirakawa and K. Maruoka, *Angew. Chem., Int. Ed.*, 2013, **52**, 4312–4348; (e) T. Ooi and K. Maruoka, *Angew. Chem., Int. Ed.*, 2007, **46**, 4222–4266.

15 (a) R. Mohammadzadeh Kakhki, *J. Inclusion Phenom. Macrocyclic Chem.*, 2013, **75**, 11–22; (b) A. Späth and B. König, *Beilstein J. Org. Chem.*, 2010, **6**, 32; (c) P. Mateus, N. Bernier and R. Delgado, *Coord. Chem. Rev.*, 2010, **254**, 1726–1747; (d) G. W. Gokel, W. M. Leevy and M. E. Weber, *Chem. Rev.*, 2004, **104**, 2723–2750; (e) S. M. Khopkar, *Analytical Chemistry of Macrocyclic and Supramolecular Compounds*, Springer-Verlag, Berlin, 2002; (f) J. S. Bradshaw and R. M. Izatt, *Acc. Chem. Res.*, 1997, **30**, 338–345; (g) H. An, J. S. Bradshaw and R. M. Izatt, *Chem. Rev.*, 1992, **92**, 543–572; (h) I. M. Kolthoff, *Anal. Chem.*, 1979, **51**, 1–22.

16 V. Martí-Centelles, M. D. Pandey, M. I. Burguete and S. V. Luis, *Chem. Rev.*, 2015, **115**, 8736–8834.

17 (a) C. Tortoreto, T. Achard, L. Egger, L. Guénée and J. Lacour, *Org. Lett.*, 2016, **18**, 240–243; (b) M. Austeri, D. Rix, W. Zeghida and J. Lacour, *Org. Lett.*, 2011, **13**, 1394–1397.

18 D. Poggiali, A. I. Poblador-Bahamonde and J. Lacour, manuscript in preparation.

19 D. Poggiali, A. Homberg, T. Lathion, C. Piguet and J. Lacour, *ACS Catal.*, 2016, **6**, 4877–4881.

20 A. Homberg, D. Poggiali, M. Vishe, C. Besnard, L. Guénée and J. Lacour, *Org. Lett.*, 2019, **21**, 687–691.

21 (a) M. Vishe, R. Hrdina, A. I. Poblador-Bahamonde, C. Besnard, L. Guénée, T. Bürgi and J. Lacour, *Chem. Sci.*,



2015, **6**, 4923–4928; (b) B. R. Kim, H.-G. Lee, S.-B. Kang, G. H. Sung, J.-J. Kim, J. K. Park, S.-G. Lee and Y.-J. Yoon, *Synthesis*, 2012, **44**, 42–50.

22 With macrocycles not based on the 1,4-dioxane skeleton, water molecules are not complexed in the final products.

23 A. Homberg, E. Brun, F. Zinna, S. Pascal, M. Górecki, L. Monnier, C. Besnard, G. Pescitelli, L. Di Bari and J. Lacour, *Chem. Sci.*, 2018, **9**, 7043–7052.

24 A. Homberg, R. Hrdina, M. Vishe, L. Guénée and J. Lacour, *Org. Biomol. Chem.*, 2019, **17**, 6905–6910.

25 E. Brun, K.-F. Zhang, L. Guénée and J. Lacour, *Org. Biomol. Chem.*, 2020, **18**, 250–254.

26 S. K. Ray, A. Homberg, M. Vishe, C. Besnard and J. Lacour, *Chem.–Eur. J.*, 2018, **24**, 2944–2951.

27 C. J. Pedersen and H. K. Frensdorff, *Angew. Chem., Int. Ed.*, 1972, **11**, 16–25.

28 (a) J. Yin, Y. Hu and J. Yoon, *Chem. Soc. Rev.*, 2015, **44**, 4619–4644; (b) J. F. Callan, A. P. de Silva and D. C. Magri, *Tetrahedron*, 2005, **61**, 8551–8588; (c) L. Prodi, F. Bolletta, M. Montalti and N. Zaccheroni, *Coord. Chem. Rev.*, 2000, **205**, 59–83; (d) M. H. Keefe, K. D. Benkstein and J. T. Hupp, *Coord. Chem. Rev.*, 2000, **205**, 201–228; (e) B. Valeur and I. Leray, *Coord. Chem. Rev.*, 2000, **205**, 3–40; (f) C. Bargossi, M. C. Fiorini, M. Montalti, L. Prodi and N. Zaccheroni, *Coord. Chem. Rev.*, 2000, **208**, 17–32; (g) A. J. Bryan, A. P. de Silva, S. A. De Silva, R. A. D. D. Rupasinghe and K. R. A. S. Sandanayake, *Biosensors*, 1989, **4**, 169–179.

29 (a) B. Wang and E. V. Anslyn, *Chemosensors: Principles, Strategies, and Applications*, John Wiley & Sons, 2011; (b) P. Thordarson, *Chem. Soc. Rev.*, 2011, **40**, 1305–1323.

30 F. M. Winnik, *Chem. Rev.*, 1993, **93**, 587–614.

31 M. Vishe, T. Lathion, S. Pascal, O. Yushchenko, A. Homberg, E. Brun, E. Vauthay, C. Piguet and J. Lacour, *Helv. Chim. Acta*, 2018, **101**, e1700265.

32 S. Sinn, F. Biedermann, M. Vishe, A. Aliprandi, C. Besnard, J. Lacour and L. De Cola, *ChemPhysChem*, 2016, **17**, 1829–1834.

33 A. Aster, G. Licari, F. Zinna, E. Brun, T. Kumpulainen, E. Tajkhorshid, J. Lacour and E. Vauthay, *Chem. Sci.*, 2019, **10**, 10629–10639.

34 F. Zinna, S. Voci, L. Arrico, E. Brun, A. Homberg, L. Bouffier, T. Funaioli, J. Lacour, N. Sojic and L. Di Bari, *Angew. Chem., Int. Ed.*, 2019, **58**, 6952–6956.

